Thermochimica Acta, 220 (1993) 131–150
Elsevier Science Publishers B.V., Amsterdam

Reliability of kinetic measurements for the thermal dehydration of lithium sulphate monohydrate. Part 2. Thermogravimetry and differential scanning calorimetry

Michael E. Brown [a,*], Andrew K. Galwey [b] and Alain Li Wan Po [c]

[a] *Chemistry Department, Rhodes University, Grahamstown 6140 (South Africa)*
[b] *School of Chemistry, Queen's University, Belfast BT9 5AG, Northern Ireland (UK)*
[c] *School of Pharmacy, Queen's University, Belfast BT9 5AG, Northern Ireland (UK)*

(Received 29 September 1992; accepted 22 October 1992)

Abstract

There is a great need for objective assessments of the quality, reliability and significance of kinetic data obtained for thermal decompositions of solids. In the first part of this study, kinetic parameters for the thermal dehydration of single crystal and powdered samples of lithium sulphate monohydrate ($Li_2SO_4 \cdot H_2O$) derived from isothermal measurements of the pressure of water vapour evolved in an initially evacuated, constant-volume apparatus, were examined critically. In this complementary study, kinetic parameters derived from thermogravimetry (TG) and differential scanning calorimetry (DSC), in both isothermal and programmed-temperature modes, are compared with the earlier results.

The reproducibilities of the several techniques have been examined and the problems of calibration of TG instruments in the low-temperature region are discussed.

Arrhenius parameters are compared with previously published values, and parameters from isothermal measurements are compared with those obtained using programmed-temperature measurements. Differences in behaviour arising from different sample preparations and from the different experimental techniques are discussed.

INTRODUCTION

The present study has been undertaken to provide objective assessments of the quality, reliability and significance of measured kinetic data for thermal decompositions of solids. The dehydration of lithium sulphate monohydrate was selected as an appropriate representative reaction for comparative investigations. The stoichiometry is simple: reaction is completed in a single rate process

$$Li_2SO_4 \cdot H_2O(s) \rightarrow Li_2SO_4(s) + H_2O(g) \quad (1)$$

and has been the subject of many previous studies [1–12].

* Corresponding author.

In the first part of the present programme [1], we reported a kinetic analysis of the rate equations which described the time dependence of the yield of product water vapour during isothermal dehydration in an initially evacuated, constant-volume apparatus. The present article reports further kinetic data obtained across the widest practicable temperature range using isothermal and non-isothermal thermogravimetric (TG) and differential scanning calorimetric (DSC) methods. Data were tested for conformity to those solid-state rate expressions [2] that were identified in Part 1 [1] as giving the most accurate fits to curves of fractional reaction α against time (isothermal) and temperature (non-isothermal).

EXPERIMENTAL

Reactant salt $Li_2SO_4 \cdot H_2O$

Sample A, single crystals and crushed powder (<150 μm), was from the same preparation as studied in Part 1 [1].

Sample B, Schering-Khalbaum, was used as supplied and after re-crystallization; some samples were crushed <250 μm. The results for sample B could then be compared with those for sample A. This variation in origin and treatment of the reactant is particularly relevant because of the proposed use of $Li_2SO_4 \cdot H_2O$ as a reference material for kinetic studies [13]. In addition to the TG and DSC measurements, sample B was also studied by measurements of the pressure of evolved water vapour. These comparisons enabled any differences in behaviour arising from variations of experimental techniques to be considered.

Apparatus

Thermogravimetry, TG

A Perkin-Elmer TGA-7 thermobalance, interfaced to an IBM-compatible computer and calibrated with magnetic standards, was used. Problems of accurate temperature calibration at the relatively low temperatures required for dehydration are discussed below. Flowing nitrogen was used as purge gas and samples were heated in open platinum pans.

Differential scanning calorimetry, DSC

Three similar Perkin-Elmer DSC-7 instruments were used in both isothermal and linear temperature increase modes. All experiments were conducted in a nitrogen flow, with the samples in unsealed aluminium pans. A few comparative experiments were done using sealed sample pans. Software was as supplied by Perkin-Elmer.

Data processing

Kinetic data were analysed after importing the data files into LOTUS 123 spreadsheets. Values of α were calculated as fractions of the total mass loss in TG experiments, or from the partial areas of the dehydration endotherms in DSC experiments. Examination of the linearity of plots of the integrated rate equations, $f(\alpha)$ against time, (see method 1, table 1 of ref. 1) was used to assess the precision of the fit of data to the R3 (contracting volume) and F1 (first-order) models, identified previously [1] as being the most appropriate kinetic descriptions of the dehydration behaviour.

General approach

Each of the experimental techniques used has its limitations.

The pressure apparatus [1] operates at low pressures (0–10 Torr) and the pressure of product water increases during the course of an experiment. The temperature sensor is fairly remote from the sample, but the furnace is large and temperatures are relatively uniform (error ±1 K).

Thermogravimetry with an open pan and small sample ensures efficient diffusive escape of product water, but temperature calibration is a serious problem, especially at the low end of the range used in these experiments.

Isothermal DSC in covered, but unsealed pans should permit the unhampered removal of product water. Temperature readings, after calibration, should be the most reliable of the three techniques. The temperature interval over which measurments can be made is limited at the lower end by the necessity of providing a signal that can be distinguished reliably from the base line. The upper limit requires that the signal can be distinguished from switching disturbances, which were corrected throughout our experiments by subtracting the signal measured in a blank run.

The approach in the present paper was to compare first the dehydration rates and kinetic characteristics of the two samples of the salt studied. Secondly, we have considered, where possible, the individual behaviour of each sample when the technique used for measuring the course of the dehydration was varied. Finally, we attempted to distinguish those differences which arise from sample variations from those that result from variations in the measurement technique.

RESULTS AND DISCUSSION

Comparison of dehydration rates of Samples A and B in the evolved water pressure apparatus

A series of dehydration rate measurements for Sample B crystals was made in the pressure apparatus previously used in Part 1 [1]. The shapes of

TABLE 1

Comparison of kinetic parameters obtained in the evolved water pressure experiments on Sample A and B crystals

	Sample A	Sample B
	$0.01 < \alpha < 0.99$	$0.1 < \alpha < 0.9$
Model R3		
E_a/(kJ mol^{-1})	106.3 ± 7.0	100.6 ± 5.3
ln(A/s^{-1})	24.07 ± 0.29	22.07 ± 0.28
$k_{370\,K}$/(10^{-4} s^{-1})	0.280 ± 0.029	0.241 ± 0.027
r^2	0.9392	0.9709
Model R2		
E_a/(kJ mol^{-1})	105.3 ± 6.7	100.6 ± 5.4
ln(A/s^{-1})	23.94 ± 0.28	22.27 ± 0.29
$k_{370\,K}$/(10^{-4} s^{-1})	0.339 ± 0.038	0.298 ± 0.034
r^2	0.9488	0.9695
Model F1		
E_a/(kJ mol^{-1})	109.7 ± 7.9	100.9 ± 5.3
ln(A/s^{-1})	26.75 ± 0.32	23.67 ± 0.28
$k_{370\,K}$/(10^{-4} s^{-1})	1.35 ± 0.15	1.07 ± 0.11
r^2	0.9285	0.9710

the α versus time curves were deceleratory, as found for Sample A, but the approach to completion, $\alpha = 1.00$, was more protracted and so the deceleratory models, R3, R2 and F1, did not give as good a description of the course of reaction over a wide range of α. The curves were, however, analysed for conformity to these models over the decreased range of $0.1 < \alpha < 0.9$ and the rate coefficients were used to calculate the Arrhenius parameters which are compared with those for Sample A crystals ($0.01 < \alpha < 0.99$) [1] in Table 1.

It should be noted that throughout this paper and Part 1 [1], the integration constants 2 and 3 for R2 and R3, respectively, were not used in the calculation of the corresponding rate coefficients, e.g. $1 - (1 - \alpha)^{1/2} = k'(t - t_0)$ where $k' = k/2$. The effect of using k in place of k' would be to add 0.69 to $\ln A$ for R2 and 1.10 for R3. Values of activation energies are not affected. The comparison of application of an individual model is consistent from sample to sample.

The results in Table 1 confirm that there is no great difference in the kinetic behaviour of the two samples under the dehydration conditions of the pressure apparatus. Some differences are to be expected from particle-size distribution effects as already discussed in Part 1 [1] for single crystal and powdered fractions of the same sample.

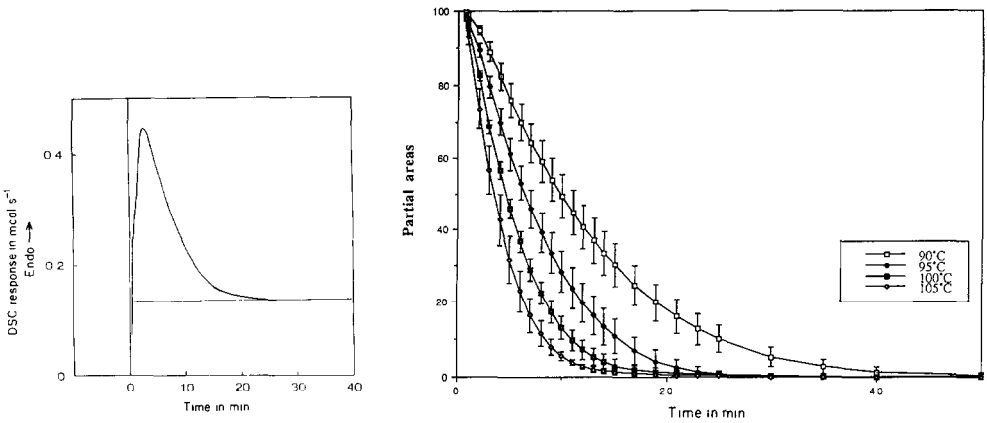

Fig. 1. (a) Typical isothermal DSC trace for the dehydration of lithium sulphate monohydrate, Sample A powder at 373 K. (b) Means of four isothermal DSC runs at four different temperatures.

Comparison of water pressure and isothermal DSC measurements on Sample A powder

Isothermal DSC experiments were possible from 363 to 378 K. A typical trace, showing the endothermic response, is given in Fig. 1(a). Values of the fractional reaction α were calculated from the partial areas of the endotherm at selected t values (Fig. 1(b)). The (α, t) data calculated in this way were then analysed, as above, by examining the linearity of the $f(\alpha)$ versus time plots. The reproducibility of the technique is illustrated by the variations in the rate coefficients (k/s^{-1}) listed in Table 2, calculated from the least-squares line through the plots of $f(\alpha)$ against t for the R3, R2 and F1 models. The R3 model gave the best fit over the range $0 < \alpha < 0.90$, followed by R2, which was in turn better than F1.

The Arrhenius plot for the above results gave the parameters listed in Table 3. These parameters are compared with the values obtained [1] for Sample A powder in the pressure apparatus. Combination of the two sets of results gave the plot shown in Fig. 2 (for the F1 model), and the parameters listed in Table 3.

Rate coefficients for the dehydration of Sample A powder, obtained using the two different techniques, lie on a single Arrhenius plot, although the isothermal DSC results show more scatter. This is evidence that the temperature calibrations for both systems are consistent.

Isothermal DSC on Sample B crystals

Isothermal DSC experiments on Sample B crystals were carried out at temperatures in the range 363–413 K. A typical trace is shown in Fig. 3 (for

TABLE 2

Reproducibility of isothermal DSC experiments on lithium sulphate monohydrate powder (Sample A) ($0 < \alpha < 0.90$)

T/K	Rate coefficients/(10^{-4} s^{-1})		
	R3	R2	F1
363	3.33	4.03	16.83
363	3.85	4.42	23.00
363	3.07	3.75	14.50
363	3.98	4.45	25.50
Av.	3.56	4.16	19.96
Std. dev.	0.43	0.34	5.15
%	12.1%	8.2%	25.8%
368	5.15	6.65	21.50
368	7.38	8.65	40.50
368	6.55	7.97	31.33
368	6.08	7.55	28.00
Av.	6.29	7.71	30.33
Std. dev.	0.93	0.84	7.91
%	14.8%	10.9%	26.1%
373	7.73	9.65	34.83
373	8.13	10.07	37.50
373	8.87	10.72	43.50
373	10.00	11.60	55.33
Av.	8.86	10.51	42.79
Std. dev.	1.00	0.85	9.11
%	11.5%	8.1%	21.3%
378	8.02	9.15	44.83
378	9.68	10.60	63.83
378	9.38	10.35	59.83
378	8.33	9.17	51.67
Av.	8.85	9.82	55.04
Std. dev.	0.80	0.77	8.48
%	9.1%	7.8%	15.4%

a 15.72 mg sample at 373 K in N_2), together with the α-time curve obtained by integration. The R3 model was acceptable at low T and the F1 model at high T, with the R2 model being accpetable in between. The reproducibility of the kinetic behaviour is illustrated by the values of the rate coefficients $k/10^{-4}$ s^{-1} based on the F1 model for three runs at 393 K (r^2 values in parentheses for $0.01 < \alpha < 0.99$): 6.06 ± 0.01 (0.9974), 8.57 ± 0.03 (0.9989) and 8.24 ± 0.01 (0.9987). Recrystallized sample B, under the same conditions, gave 8.35 ± 0.04 (0.9882) which is not significantly different.

TABLE 3

Comparison of kinetic parameters obtained from evolved water pressure experiments and isothermal DSC measurements on Sample A, powder

	Water pressure apparatus	Isothermal DSC	Combined
Model R3			
E_a/(kJ mol^{-1})	87.0 ± 5.7	70.3 ± 9.2	90.8 ± 3.0
ln(A/s^{-1})	20.71 ± 0.33	15.48 ± 0.18	22.06 ± 0.28
$k_{370\,K}$/(10^{-4} s^{-1})	5.13 ± 0.86	6.24 ± 0.25	5.87 ± 0.36
r^2	0.9317	0.8061	0.9655
Model R2			
E_a/(kJ mol^{-1})	85.2 ± 5.9	66.3 ± 10.0	89.5 ± 3.1
ln(A/s^{-1})	20.26 ± 0.34	14.33 ± 0.20	21.80 ± 0.30
$k_{370\,K}$/(10^{-4} s^{-1})	5.9 ± 1.0	7.38 ± 0.32	6.89 ± 0.44
r^2	0.9255	0.7581	0.9611
Model F1			
E_a/(kJ mol^{-1})	91.7 ± 5.6	78.7 ± 10.9	94.8 ± 3.0
ln(A/s^{-1})	23.94 ± 0.32	19.88 ± 0.21	25.05 ± 0.28
$k_{370\,K}$/(10^{-4} s^{-1})	28.1 ± 4.6	32.9 ± 1.6	31.4 ± 1.9
r^2	0.9413	0.7894	0.9686

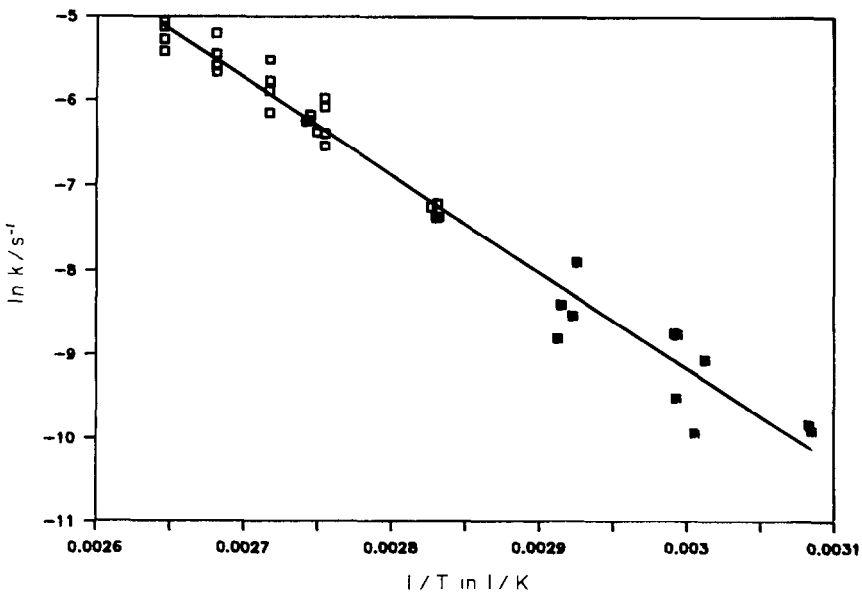

Fig. 2. Arrhenius plot for Sample A powder using combined pressure apparatus and isothermal DSC results: □, pressure apparatus; ■, isothermal DSC.

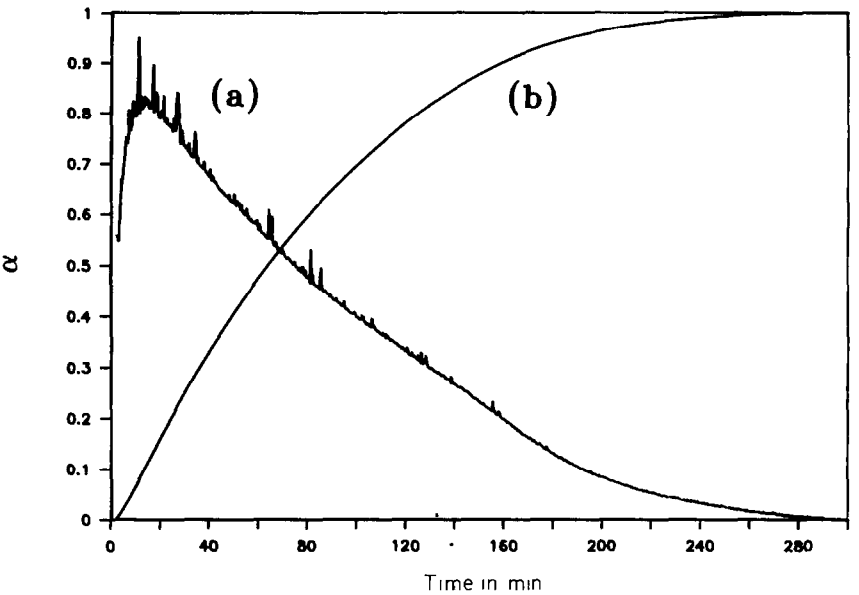

Fig. 3. Typical isothermal DSC trace for the dehydration of lithium sulphate monohydrate, Sample B crystals at 373 K. Curve, (a) DSC response (scaled); curve (b) α versus time.

The mean of all four values with the standard deviation is $(7.55 \pm 1.06) \times 10^{-4}\,s^{-1}$.

An Arrhenius plot of the isothermal DSC results for Sample B crystals, using the F1 model and all the k values measured, gave $E_a = 48.2 \pm 6.2$ (12.9%) kJ mol^{-1} and $\ln(A/s^{-1}) = 7.50 \pm 0.21$ ($r^2 = 0.8972$). Omission of the 363 K point, where the fit of the F1 model was poor, increased the E_a value to 56.6 ± 7.8 (13.8%) kJ mol^{-1} and $\ln(A/s^{-1})$ increased to 10.03 ± 0.19 ($r^2 = 0.8979$).

The Arrhenius plot for the isothermal DSC results was combined with that obtained from the pressure apparatus results above (both sets of data are for Sample B), as shown in Fig. 4 (for model F1). The value of E_a was 94.8 ± 3.0 kJ mol^{-1} and $\ln(A/s^{-1})$ was 25.05 ± 0.28 ($r^2 = 0.9687$) (see Table 3). It is clear that deviations of the two sets are within experimental error over the major portion of the temperature range and only become marked at the extremes. Results at low temperatures, using both techniques, may be influenced by some contribution from the reverse reaction.

Isothermal TG experiments on Sample B crystals

Three series of isothermal TG runs on Sample B crystals were carried out. A major problem in TG is temperature calibration, especially at the low end of the temperature range. Each series of experiments followed different attempts at magnetic calibration of the furnace, based on two

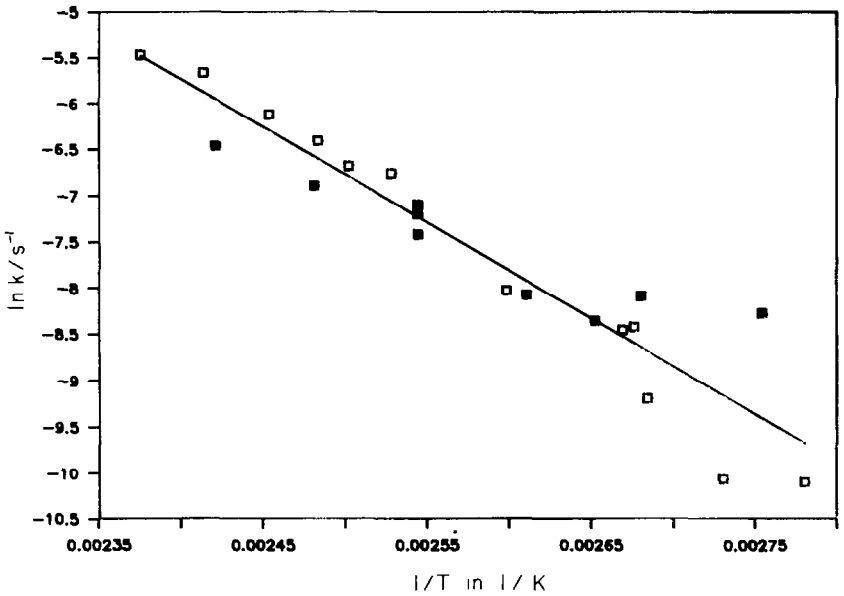

Fig. 4. Arrhenius plot for Sample B crystals using combined pressure apparatus and isothermal DSC results. □, pressure apparatus; ■, isothermal DSC.

Curie points (alumel, 436 K and nickel, 627 K), and adjustments of the position of the sample in the furnace.

The average mass losses from the TG experiments were: crystals (323–393 K) 13.32 ± 0.57%, and powder (323–373 K) 13.76 ± 0.43%. These values are slightly less than expected (14.07%) for complete dehydration according to eqn. (1).

The α versus time curves calculated from the isothermal TG curves (at nominal temperatures from 323 to 393 K) were similar in their overall features to the results obtained [1] in the accumulatory water vapour pressure apparatus. Any acceleratory contribution was within the time required for heating to reaction temperature. Typical α versus time and $d\alpha/dt$ versus time plots are shown in Fig. 5 (nominal 363 K from Series 3). It was not always possible to distinguish clearly which of the models R3 or F1 gave the better description of the kinetics of dehydration.

The kinetic parameters obtained from Arrhenius plots, based on rate coefficients for the F1 model, for the three different series are given in Table 4.

These values are not consistent within the technique (TG) and are significantly different from the values obtained (above) for Sample B crystals in the pressure apparatus ($E_a/(\text{kJ mol}^{-1}) = 78.7$, $\ln(A/\text{s}^{-1}) = 19.88$) and from the combined set from the pressure apparatus and the isothermal DSC ($E_a/(\text{kJ mol}^{-1}) = 94.8$, $\ln(A/\text{s}^{-1}) = 25.05$). These differences must arise from differences in the environment experienced by the sample, and

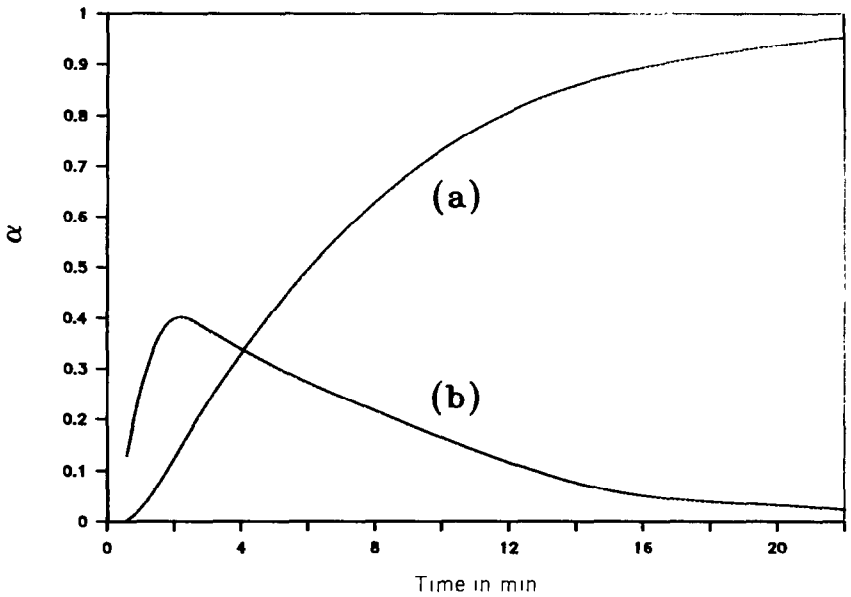

Fig. 5. Curve (a) α versus time and curve (b) $d\alpha/dt$ versus time (scaled $\times 25$) from isothermal TG runs on Sample B crystals at 363 K.

uncertainty in the temperature calibration is the most obvious factor. Temperature calibration may be in error in at least two ways: (1) a constant displacement of the scale ($\Delta T = C_0$) from its true value, and (2) a variable displacement of the scale ($\Delta T = f(T)$) which is itself T dependent.

To estimate the temperature inaccuracies, it was assumed that the calibration of the T scale in each of the TG series was in error by an

TABLE 4

Kinetic parameters for isothermal TG dehydration experiments on Sample B crystals using the F1 model

	Series 1	Series 2	Series 3
Model F1			
$E_a/(\text{kJ mol}^{-1})$	69.9 ± 8.8	60.5 ± 5.0	84.4 ± 4.5
$\ln(A/\text{s}^{-1})$	14.82 ± 0.22	10.75 ± 0.19	22.02 ± 0.29
$k_{370\,\text{K}}/(10^{-4}\,\text{s}^{-1})$	3.70 ± 0.73	1.35 ± 0.29	43.7 ± 4.4
r^2	0.9564	0.9547	0.9746
T^*/K [a]	346	336	374
$\Delta T/\text{K}$ [b]	24	34	−4

[a] T^* is the temperature on the reference Arrhenius plot (see text) which would give the rate coefficient measured here as k_{370}.

[b] ΔT is the temperature calibration error = 370 − T^*.

amount, ΔT_i, relative to that in the combined pressure apparatus and isothermal DSC set (the reference Arrhenius plot). ΔT_i was further assumed to be constant in each series, but to vary between each series with the detailed calibration procedure (see above). ΔT_i was estimated by calculating the temperature T^* on the reference Arrhenius plot which would give the value of the rate coefficient, k^*_{370}, corresponding to the apparent temperature of 370 K on the actual plot, i.e.

$$T^* = (E_a/R)(\ln A - \ln k^*_{370})$$

ΔT_i is then $370 - T^*$. Values of T^* and ΔT_i are given in Table 4. ΔT_i ranges from 15 to 35 K. In the configuration used in Series 2, a thermocouple was inserted in the sample position in the furnace and its readings were from 20 to 30 K below the set temperature from 323 to 403 K.

Isothermal TG experiments on Sample B powder

Sample B crystals were ground to a powder, less than 250 μm mesh. The α versus time curves for these powder samples were more complex than those of the crystals; compare the α versus t plots of Figs. 5 and 6. Plots of $d\alpha/dt$ versus t showed the existence of at least two overlapping stages: there was a dominant rapid reaction superimposed on a slower process, with relative rate maxima of 6:1. This change in dehydration behaviour with particle size is discussed below.

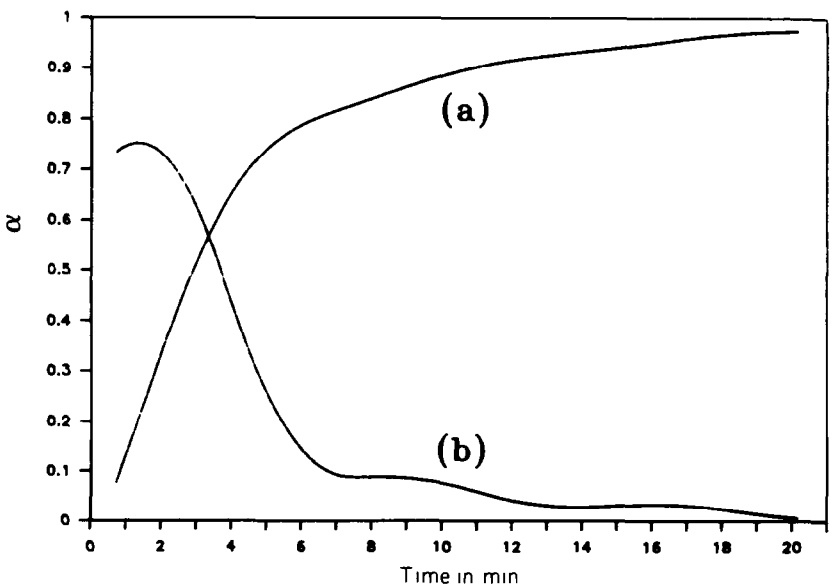

Fig. 6. Curve (a) α versus time and curve (b) $d\alpha/dt$ versus time (scaled $\times 25$) from isothermal TG runs on Sample B powder at 363 K.

PROGRAMMED-TEMPERATURE EXPERIMENTS

Kinetic analysis

Numerous methods have been proposed for the extraction of kinetic parameters from programmed-temperature experiments. A simple method often used is that originally proposed by Borchardt and Daniels (BD) [14]. The BD method is based on the isothermal rate equation

$$d\alpha/dt = kf'(\alpha) = A \exp(-E_a/RT)f'(\alpha)$$

coupled with the assumption that

$$d\alpha/dT = (d\alpha/dt)(dt/dT) = (d\alpha/dt)/\phi$$

where ϕ is the constant heating rate (dT/dt), and hence

$$k = (d\alpha/dt)/f'(\alpha) = \phi(d\alpha/dT)/f'(\alpha)$$

at temperature T. The k (based on a choice of model $f(\alpha)$) and T values are then used in a conventional Arrhenius plot. Often, but not necessarily, the model selected for trial is F1 ($f'(\alpha) = (1-\alpha)$, $n = 1$).

DSC

A typical DSC trace for the dehydration of $Li_2SO_4 \cdot H_2O$, Sample A powder (2.661 mg) in nitrogen at a heating rate of 5.0 K min^{-1} in an unsealed aluminium pan, is shown in Fig. 7. The signal at temperature T is

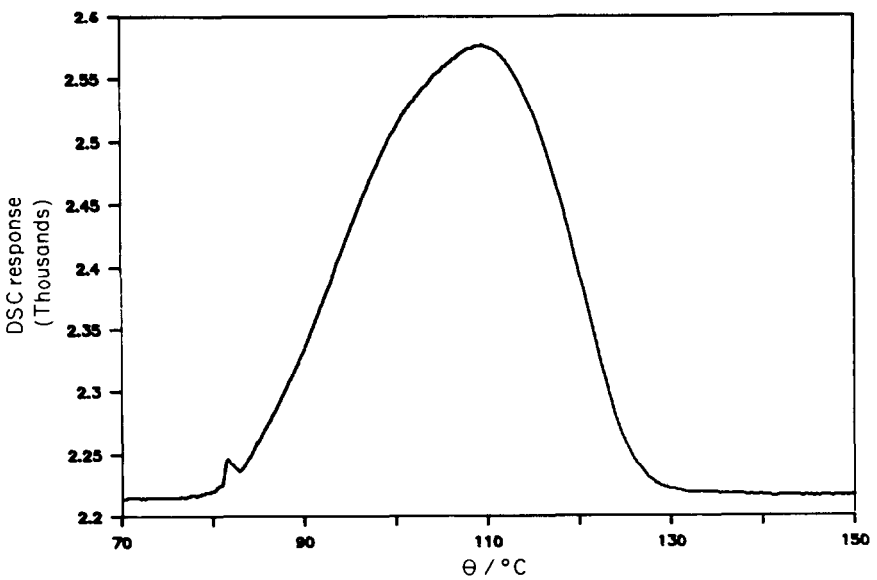

Fig. 7. Programmed temperature DSC scan for Sample A powder, at 5 K min^{-1} in N_2.

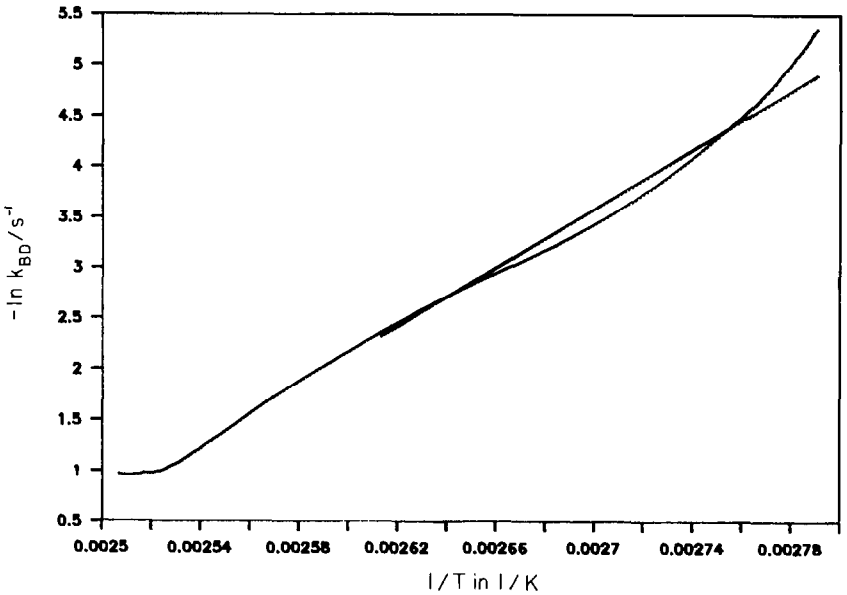

Fig. 8. Arrhenius plot (Borchardt and Daniels method) for DSC scan in Fig. 7.

assumed to be proportional to $d\alpha/dt$ and the partial area under the curve at the same temperature is assumed to be proportional to α.

For $Li_2SO_4 \cdot H_2O$ powder, the F1 model gave the most acceptable Arrhenius plot, Fig. 8. The kinetic parameters estimated from this and other such plots for experiments at other heating rates, are listed in Table 5.

A DSC scan for Sample B crystals (9.33 mg), heated at 5 K min^{-1} in N_2, is

TABLE 5

Kinetic parameters from programmed-temperature experiments on $Li_2SO_4 \cdot H_2O$

Heating rate /(K min^{-1})	T range /K	E_a/(kJ mol^{-1})	ln(A/s^{-1})	r^2
DSC, Sample A, powder				
20	368–417	120.1 ± 1.4	32.49 ± 0.20	0.9799
10	361–405	119.8 ± 1.0	32.46 ± 0.12	0.9910
5	358–400	121.2 ± 0.8	33.31 ± 0.11	0.9916
DSC, Sample B, crystals				
5	392–455	98.0 ± 0.7	21.36 ± 0.14	0.9858
TG, Sample B, crystals				
5	385–455	92.6 ± 0.6	20.34 ± 0.15	0.9869
5 [a]	365–435	84.0 ± 0.5	19.07 ± 0.15	0.9872

[a] Temperature scale corrected by −20 K.

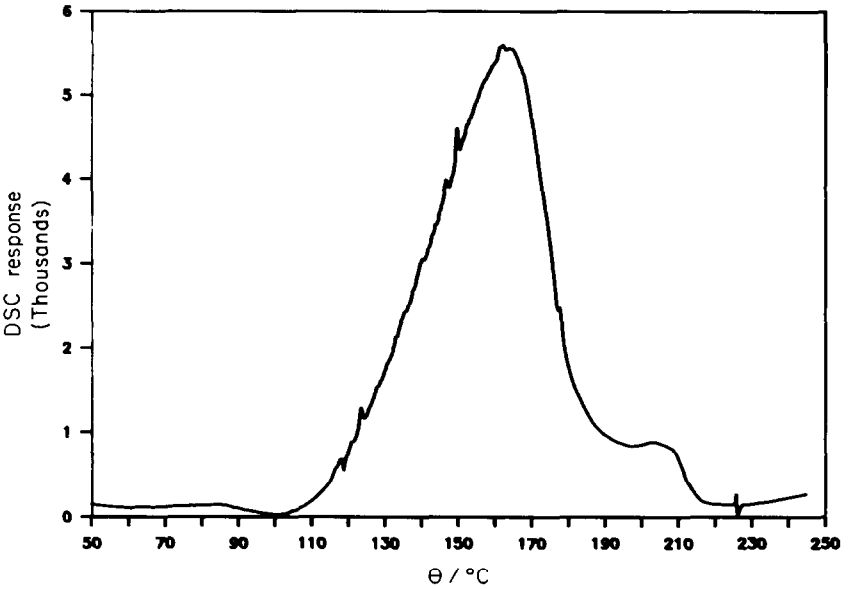

Fig. 9. Programmed temperature DSC scan for Sample B crystals, at 5 K min^{-1} in N_2.

shown in Fig. 9. Kinetic analysis, as above, gave the parameters listed in Table 5.

TG

A typical programmed-temperature TG run on Sample B crystals heated at 5 K min^{-1} in N_2 is shown in Fig. 10. The Borchardt and Daniels analysis [14], using the F1 model, gave the Arrhenius plot shown in Fig. 11 and the kinetic parameters listed in Table 5. If it was assumed that the temperature calibration was in error by −20 K, as discussed above, the calculated parameters are decreased as shown in Table 5.

In a recent study [19] of the effect of water vapour on the kinetics of the dehydration, Huang and Gallagher calculated kinetic parametes from the results of their programmed-temperature TG and DSC experiments. They used the Ozawa method [20] of kinetic analysis which is based on the comparison of the temperatures measured at fixed values of α for experiments at different heating rates.

The apparent activation energies, E_a varied most markedly with the extent of dehydration α, being high initially and dropping to more constant values above $\alpha = 0.5$. There were also differences in the E_a values with the form of the sample (powder, pellets, plate crystals, or cubic crystals) with powders having the highest E_a values (Table 6). The effect of water vapour in the purge gas on the values of E_a was relatively slight. E_a values measured in the DSC experiments were generally lower than those

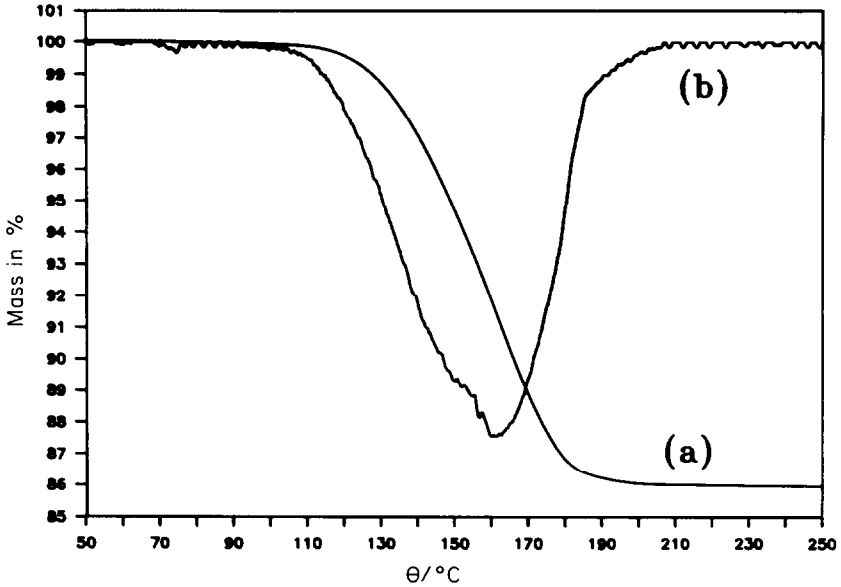

Fig. 10. Programmed temperature TG run for Sample B crystals, at 5 K min^{-1} in N_2. Curve (a) TG; curve (b) DTG.

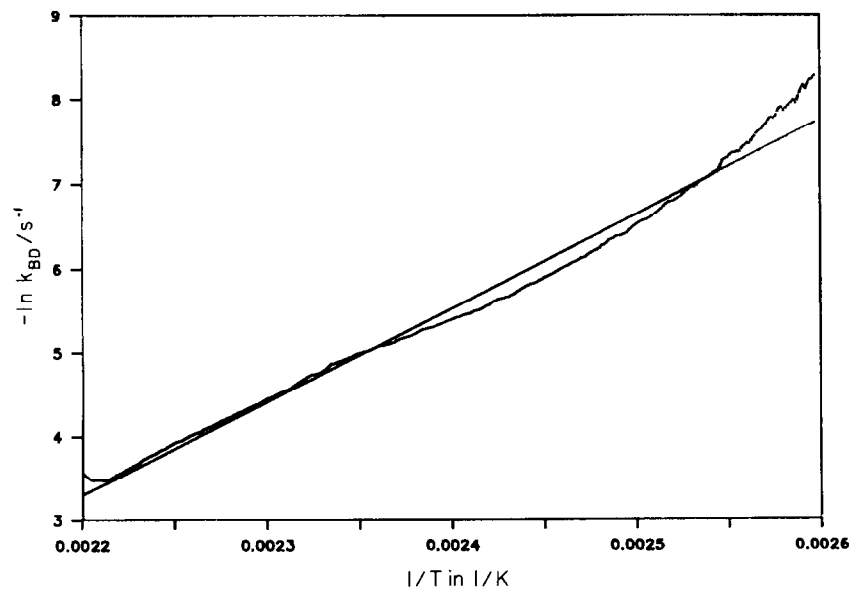

Fig. 11. Arrhenius plot (Borchardt and Daniels method) for TG run in Fig. 10.

TABLE 6

Published [19] activation energies in kJ mol^{-1} from programmed-temperature TG and DSC experiments on $Li_2SO_4 \cdot H_2O$ ($0.14 < \alpha < 0.85$)

	Dry nitrogen	Wet nitrogen
TG		
Powder	220–86	114–80
Pellets	94–61	96–71
Plate crystals	105–74	117–81
Cubic crystals	89–71	108–74
DSC		
Powder	85–73	
Pellets	72–51	
Plate crystals	78–70	
Cubic crystals	84–66	

obtained from TG measurements, and this was ascribed to the effects of constructional differences on the sample environment. Huang and Gallagher's E_a values [19] are summarized in Table 6.

CONCLUSIONS

All the α versus time plots for the dehydrations of both reactant samples showed similar overall shapes from measurements obtained using all three different experimental techniques. The short initial, apparently acceleratory period of dehydration undoubtedly contains a contribution from heat transfer effects during the heating of the reactant mass to reaction temperature. It is less clear, however, whether the initial brief acceleratory period of reaction, which has been associated [12] with the rapid (perhaps instantaneous) nucleation and early coalescence of nuclei on growth, is significant in our kinetic measurements. Establishment of a coherent reaction interface across all reactant surfaces is certainly completed at a low α value. The detailed shapes of the α versus time curves depend slightly on the experimental technique and prevailing conditions, notably including the ease of escape of product water vapour away from the reactant solid.

It was not possible to identify which of the three deceleratory kinetic expressions tested here in detail (R3, R2 or F1) gave the most satisfactory description of the main part of the dehydration. The reaction interface in the present salt is of appreciable thickness [15] so that the kinetic behaviour may not conform exactly to rate equations based on the assumption of a sharp reactant-to-product transformation [2]. A critical factor in deciding between the contracting area (R2), contracting volume (R3) and first-order (F1) models is the accuracy with which the yield corresponding to completion of reaction is known. The distinction between the alternative

models is most evident in the later stages of dehydration ($\alpha > 0.9$) where processes based on mechanisms of interface advance (R2 and R3) proceed relatively rapidly to completion, in contrast with the more extended deceleratory character of a first-order process (F1). Throughout this work (Parts 1 [1] and 2), all three rate expressions provided satisfactory representations of our data.

The reproducibility of measurements of rate coefficients was determined in experiments based on measurements of water vapour pressure in the constant volume apparatus. Variations in magnitudes are shown in table 3 of ref. 1. The scatter of values is greatest for powder samples where the particle sizes and size distributions exert a considerable influence over the rate of dehydration. Crushing markedly increases reaction rates [12], as expected for an interface reaction mechanism. The irregularities of behaviour shown in the differential curve (Fig. 6) are ascribed to overlap of the concurrent dehydrations of fractions of reactant powder containing groups of particles of different dimensions.

Arrhenius parameters from the present work (Parts 1 [1] and 2), together with selected values from other authors, are summarized in Tables 6 and 7.

TABLE 7

Summary of kinetic parameters for dehydration of lithium sulphate monohydrate (see also Table 6)

	Present work and ref. 1			Other workers		
	A crystals	B crystals	A powder	Crystals	Powder	Ref.
Pressure apparatus						
E_a/(kJ mol^{-1})	105–110	101	85–92	80	92	12
ln(A/s^{-1})	24–27	22–24	20–24	16	23	
Isothermal DSC						
E_a/(kJ mol^{-1})		57	66–79			
ln(A/s^{-1})		10	14–20			
Isothermal TG						
E_a/(kJ mol^{-1})		61–84 [a]		112		10
ln(A/s^{-1})		10.8–22.0		26.0		
Programmed T DSC						
E_a/(kJ mol^{-1})		98	120	92	137	16,17
ln(A/s^{-1})		21	33	18.9	36.4	
Programmed T TG						
E_a/(kJ mol^{-1})		93		93	135	16,17
ln(A/s^{-1})		20		19.3	35.7	

[a] See text for temperature calibration problems.

Isothermal DSC and pressure measurements for crushed powder Sample A gave rate coefficients that were close to a single line on the Arrhenius plot, Fig. 2. Thus we find no problem in relating rate observations for powder dehydrations by both techniques. Observations for Sample B single crystals were less satisfactory, Fig. 4. Data were close to a single line in the middle of the temperature range, but diverged at both the upper and lower ends of the range studied. Reactivities of the salt were comparable but the pressure apparatus gave a high activation energy (105–110 kJ mol^{-1}, greater than the value for powder) while isothermal DSC gave a value that was little more than half (57 kJ mol^{-1}). Reasons for the low value for isothermal DSC (compared with programmed-temperature DSC measurements, Table 7) have not been characterized, but may arise from errors in defining the base line in the absence of sample.

Kinetic parameters obtained from isothermal TG measurements were very sensitive to the temperature calibration procedure. It was shown that directly determined temperatures in the reaction zone were in error by up to 35 K, compared to values obtained using two-point magnetic calibration. The consequences of this deviation were evidently less significant in programmed-temperature TG experiments where Arrhenius parameters were in closer agreement with values obtained from isothermal experiments (Table 7). This uncertainty, however, remains throughout the TG studies.

The Arrhenius parameters in Table 7 exhibit compensation behaviour [2, 18], see Fig. 12. The points can either be regarded as somewhat scattered

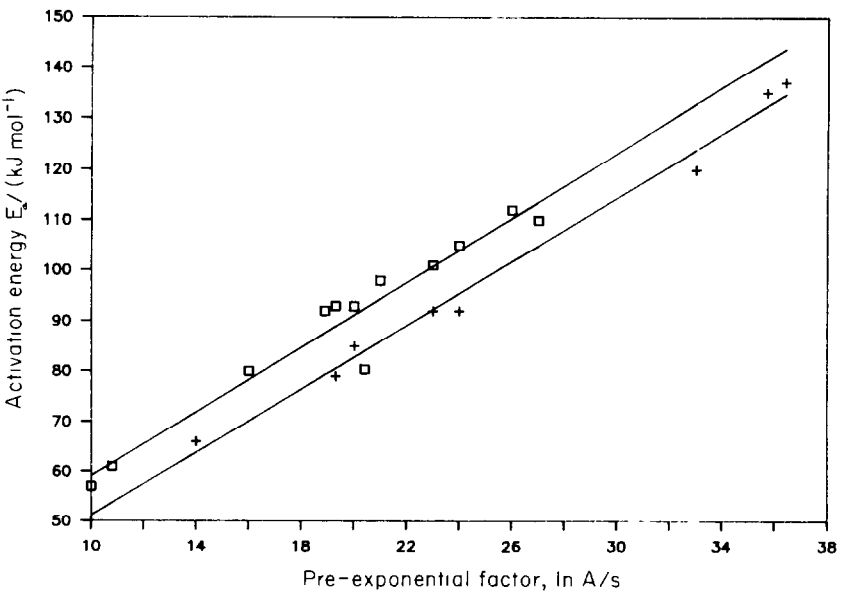

Fig. 12. Compensation plot for the dehydration of $Li_2SO_4 \cdot H_2O$, based on the Arrhenius parameters in Table 6. □, crystal; +, powder.

about a single line or as being grouped about two parallel lines, applicable to single crystal and crushed powder samples. Representation of the data by two lines identifies an increase in rate for powder samples as an increase in pre-exponential factor arising from the greater area of the powdered particles from which water is lost. This example of compensation behaviour is found for the same reaction occurring in comparable temperature intervals. Because the chemical change is constant, we must conclude that the compensating variations in $\ln A$ and E_a arise through unidentified inconsistencies in measurement methods and do not have mechanistic significance.

We summarize our conclusions from the studies (Parts 1 [1] and 2) of the kinetics and mechanism of $Li_2SO_4 \cdot H_2O$ dehydration as follows.

1. The reactivities of all samples were comparable. The present kinetic measurements were completed within similar temperature ranges, though reactions of powders were relatively more rapid. The reverse reaction (rehydration) exerted little, if any, influence on dehydration kinetics, except at the lowest temperatures [12].

2. Although dehydration has been identified as a nucleation and growth process [12] and occurs at an advancing interface [15], kinetic data did not conform to rate equations (R2 and R3), based on interface advance, with greater precision than to the first-order expression (F1). An initial nucleation stage in the reaction was not easily characterized from yield–time measurements. Kinetic measurements do not, therefore, readily provide mechanistic information about the changes of interface geometry as water loss proceeds. One probable explanation is the appreciable thickness of the dehydration layer [15]. The variation in the extent of water loss across this zone means that the geometric model is not strictly applicable, particularly for the smaller reactant crystallites. Furthermore, water losses from the internuclear surface regions during the earliest stages of dehydration will obscure the acceleratory process [12] characteristically associated with nucleation [2]. As is usual in the field [2], the interpretation of rate data requires the support of other observations, microscopy being particularly useful.

3. Probably the most unsatisfactory feature of the present study was the large range of A and E values measured for the same reaction of several samples of salt by different techniques. Even discounting the more extreme values (Tables 6 and 7), it is difficult to place confidence in the individual values of Arrhenius parameters measured. From the results reported we cannot identify a preferred value of E for this reaction, possibly the most reliable results are 80–100 kJ mol^{-1}. This is hardly a precise conclusion from one of the most intensively and extensively investigated dehydration reactions studied recently.

We cannot, therefore, recommend $Li_2SO_4 \cdot H_2O$ for use as a reference material for the standardization of kinetic measurements.

REFERENCES

1 M.E. Brown, A.K. Galwey and A. Li Wan Po, Thermochim. Acta, 203 (1992) 221.
2 M.E. Brown, D. Dollimore and A.K. Galwey, Comprehensive Chemical Kinetics, Vol. 22, Elsevier, Amsterdam, 1980.
3 V.G. Vasilev and Z.V. Ershova, Russ. J. Phys. Chem., 46 (1972) 1197.
4 G. Thomas and M. Soustelle, J. Chim. Phys., 69 (1972) 1770.
5 G. Bertrand, M. Lallemant and G. Watelle-Marion, J. Inorg. Nucl. Chem., 36 (1974) 1303.
6 H. Tanaka, Thermochim. Acta, 52 (1982) 195.
7 V.B. Okhotnikov, B.J. Yacobson and N.Z. Lyakhov, React. Kinet. Catal. Lett., 23 (1983) 125.
8 Y.A. Gaponov, B.I. Kidyarov, N.A. Kirdyashkina, N.Z. Lyakhov and V.B. Okhotnikov, J. Therm. Anal., 33 (1988) 547.
9 N.A. Kirdyashkina and V.B. Okhotnikov, React. Catal. Lett., 36 (1988) 417.
10 N. Koga and H. Tanaka, J. Phys. Chem., 93 (1989) 7793.
11 V.B. Okhotnikov, N.A. Simakova and B.I. Kidyarov, React. Kinet. Catal. Lett., 39 (1989) 345.
12 A.K. Galwey, N. Koga and H. Tanaka, J. Chem. Soc. Faraday Trans., 86 (1990) 531.
13 J.H. Flynn, personal communication, 1989.
14 H.J. Borchardt and F. Daniels, J. Am. Chem. Soc., 79 (1957) 41.
15 V.V. Boldyrev, Y.A. Gaponov, N.Z. Lyakhov, A.A. Politov, B.P. Tolochko, T.P. Shaktshneider and M.A. Sheromov, Nucl. Instrum. Methods Phys. Res., A261 (1987) 192.
16 H. Tanaka and N. Koga, J. Therm. Anal., 36 (1990) 2601.
17 N. Koga and H. Tanaka, Thermochim. Acta, 185 (1991) 135.
18 A.K. Galwey, Adv. Catal., 26 (1977) 247.
19 J. Huang and P.K. Gallagher, Thermochim. Acta, 192 (1991) 35.
20 T. Ozawa, J. Therm. Anal., 2 (1970) 301.